Modeling of Dish-Stirling Solar Thermal Power Generation

Dustin Howard, *Student Member, IEEE* and Ronald G. Harley, *Fellow, IEEE*

***Abstract*--Dish-Stirling solar power generation has emerged as an efficient and reliable source of renewable energy. As the technology moves into commercialization, models become necessary to predict system behavior under various operating conditions. Current literature on dish-Stirling modeling is scattered, focusing on individual components within the system. This paper establishes a background of the individual component models, and provides a method for integration of the various component models to form a comprehensive model. The thermal, electrical, and control systems of the dish-Stirling system are presented, along with a method for simulation. Typical results are provided for the instantaneous working gas temperature, pressure, and torque, along with results indicating how these parameters vary with solar irradiance in steady state.**

***Index Terms*--AC generators, Energy conversion, Energy resources, Heat engine, Induction generators, Modeling, Simulation, Solar energy, Solar power generation, Thermoelectric energy conversion.**

I. Nomenclature

Symbol

c	specific heat capacity (J/(kg*K))
d	diameter (m)
D	derivative operator with respect to time
F	friction factor (kg*m^2/s)
gA	mass flow (kg/s)
h	heat transfer coefficient (W/(m^2*K))
I	irradiance (W/m^2)
J	moment of inertia (kg*m^2)
m	mass (kg)
M	total mass of working gas inside Stirling engine (kg)
p	working gas pressure (Pa)
Q	heat (J)
R	gas constant (m^3*Pa/(K*kg))
T	temperature (K)
V	volume (m^3)
W	work (J)
ϕ	crank angle (rad)
η	efficiency
ρ	material density (kg/m^3)
τ	torque (N*m)
ω	Shaft rotational speed (rad/s)

Subscript

a	ambient
c	compression space
ck	compression space-cooler interface
con	concentrator
d	dead space
$elec$	electric
e	expansion space
h	heater
he	heater-expansion space interface
I	Input
k	cooler
kr	cooler-regenerator interface
L	losses
m	mirror
p	constant pressure
r	regenerator
rh	regenerator-heater interface
s	swept space
v	constant volume

II. Introduction

Dish-Stirling technology development began in the late 1970's as a U.S. Department of Energy sponsored Solar Dish Electric Program with Jet Propulsion Laboratory. Currently, the technology is being developed in several locations worldwide. The most unique characteristic of this technology is the prime mover, known as a Stirling engine. The high temperatures achievable with concentrated solar energy make Stirling engines a prime candidate for solar thermal electric energy conversion, due to their high operating efficiency and emission free operation. The technology has demonstrated operating success, achieving the world's record for solar-to-grid energy conversion efficiency. Megawatt rated plants are now online, with plants rated for several hundred megawatts nearing construction [1].

As dish-Stirling technology becomes more prominent as a source of renewable and distributed energy, modeling and simulation of the systems become increasingly important to predict system behavior under various operating conditions. Current literature on the modeling of dish-Stirling technology is limited and scattered. Technical literature that exists usually focuses on the operation of individual components within the dish-Stirling system. This paper brings together the thermal, electric, and control system models of the various components within the dish-Stirling system. A background of

Manuscript received November 30, 2009. This work was supported in part by the National Science Foundation, USA, under Grant 0836017.

D. Howard and R. G. Harley are with the School of Electrical and Computer Engineering, Georgia Institute of Technology, Atlanta, GA 30332, USA (e-mail: gth653d@mail.gatech.edu; rharley@ece.gatech.edu)

978-1-4244-8357-0/10/$26.00 ©2010 IEEE

the various components is provided, along with a detailed description of the component model. In addition, a strategy for integrating the various system components into one comprehensive model is given, along with typical simulation results.

III. System Overview

An example of a dish-Stirling unit is shown in Fig. 1. The main components of interest are the concentrator, receiver, Stirling engine, and generator, where the power conversion unit (PCU) contains the Stirling engine, generator, receiver, and various control systems. The concentrator consists of mirrors arranged in the shape of a paraboloid, with the focal point at the opening of the receiver. The receiver acts as a thermal interface between the concentrated sunlight and the PCU. Conductors from the PCU generator are connected to the utility through underground cables. Rated power output of systems to date range from 8 kW to 25 kW at an irradiance level of 1000 W/m^2 [3]. The units use two-axis tracking of the sun throughout the day, returning to a stow-away position in the evening when irradiance levels become too low to produce power. Two methods for controlling the receiver temperature are currently implemented, namely, variable stroke and variable pressure control. Variable pressure control is more common and is therefore used in this analysis. Detailed technical specifications on component dimensions and operating characteristics can be found in [4] for several different dish-Stirling systems.

IV. Component Analysis

A. Concentrator

The concentrator focuses the direct normal insolation (DNI) onto the receiver, where the heat is used in the energy conversion process. The key parameters in analyzing the operation of the concentrator are the dish aperture diameter d_{con}, mirror reflectivity η_m, and irradiance I. In present designs, concentrator diameters range from 8.8 meters to 15 meters and mirror reflectivity ranges from 91% to 95% [3]. With the assumption of perfect sunlight tracking, the rate of heat transfer to the receiver from the concentrator can be approximated by

$$DQ_I = \pi\left(\frac{d_{con}}{2}\right)^2 \eta_m I \qquad (1)$$

where D is the derivative with respect to time.

B. Receiver

The receiver is a cylindrical mass that serves as the interface between the concentrator and the Stirling engine. The receiver is designed to maximize the amount of heat transferred to the Stirling engine and minimize the thermal losses. Inside the receiver at the base lies the absorber, which consists of a mesh of tubes that carry the Stirling engine working gas.

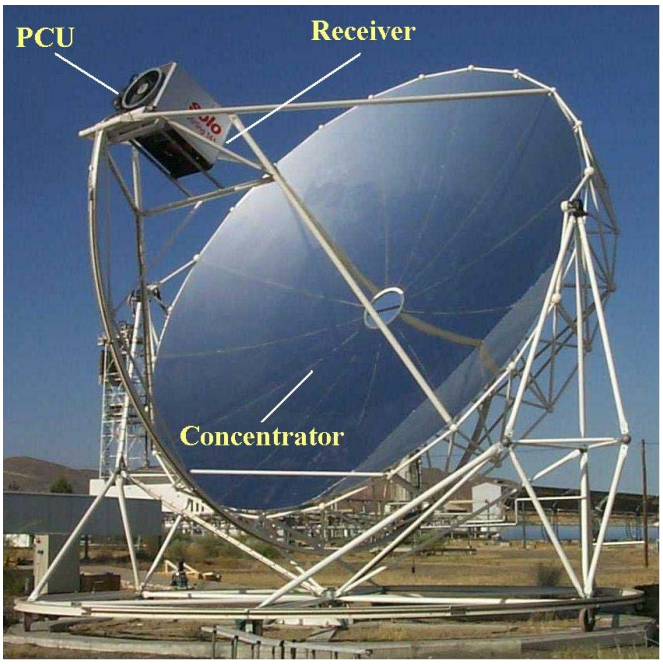

Figure 1. Dish-Stirling system with labeled components [2].

This gas flows through the mesh of tubes to absorb the heat inside the receiver to power the Stirling engine. The receiver introduces losses in the system due to thermal radiation, reflection, convective heat transfer into the atmosphere, and conduction through the receiver material [5].

Critical to the receiver operation is the temperature of the absorber. The temperature should be maintained as high as possible to maximize the efficiency of the Stirling engine, but should not exceed the thermal limits of the receiver material. Thus, the absorber temperature is a major control variable. An energy balance on the absorber yields the relation

$$\rho c_p VDT = DQ_I - DQ_L - DQ_h \qquad (2)$$

It is evident from (2) that the absorber temperature can be controlled by controlling the rate of heat transfer to the Stirling engine DQ_h. The losses in the absorber can be defined in terms of an overall loss coefficient h, and is given by

$$DQ_L = hA(T_{avg} - T_a) \qquad (3)$$

where A is a constant proportional to the receiver dimensions and T_{avg} is a temperature that characterizes the heat loss in the absorber [6].

C. Stirling Engine

The Stirling engine itself is a closed-cycle external heat engine. A working gas, usually hydrogen or helium, is contained within the engine. Two heat exchangers alternately heat and cool the working gas, thus causing expansion and compression within the working spaces of the engine. The work done in the expansion of the gas is used to drive a piston-crankshaft drive mechanism.

A simplified diagram of the Stirling engine control volumes is shown in Fig. 2. The engine contains three heat exchangers,

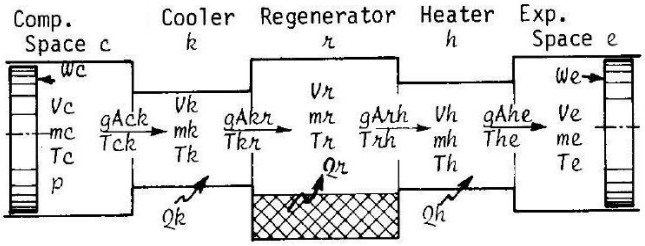

Figure 2. Heat exchangers and working spaces in a Stirling engine, with labels for the various gas parameters in each compartment (courtesy of [7]).

known as the heater, cooler, and regenerator. "Heater" is the general term used in Stirling engine literature, but represents the same mesh of tubes discussed in the previous sections known as the absorber. The working gas flows back and forth through the tubes of the heater, absorbing heat to power the Stirling engine. The regenerator is a dense wire mesh intended to recapture some of heat stored in the working gas before entering the cooler, where it will otherwise be ejected into the atmosphere. The cooler rejects excess heat to the atmosphere by various means, which can include forced air convection or water cooling. The working spaces within the engine are known as the expansion and compression spaces. The working space volumes are directly connected to the crankshaft mechanism, thus their instantaneous volumes depend on the crankshaft angle, or shaft rotational speed. The relationship between the working space volumes and crank angle is given by

$$v_{c,e} = V_d + \frac{1}{2}V_s[1+\cos(\phi - \alpha_{c,e})] \tag{4}$$

Stirling engine analysis and simulation relies on knowing the instantaneous pressure, temperature, mass, and volumes of the various spaces within the Stirling engine. The Ideal Adiabatic Model, developed by Urieli [7], provides a means of modeling the various engine parameters, with the primary assumption being adiabatic expansion and compression of the working gas in their corresponding working spaces. The model is developed by performing an energy balance on each of the heat exchanger and working space volumes, a derivation of which can be found in [8]. The resulting differential equation for the pressure, which is assumed to be uniform throughout all the engine compartments, is given by

$$Dp = \frac{\gamma RDM - \gamma p[(Dv_c/T_{ck}) + (Dv_e/T_{he})]}{[v_c/T_{ck} + \gamma(V_k/T_k + V_r/T_r + V_h/T_h) + v_e/T_{he}]} \tag{5}$$

The pressure differential equation (5) is a modified version of that given in [7] to account for the non-constant mass in the engine due to the pressure control system. The mass of working gas in the compression space is determined using the relation

$$Dm_c = \frac{pDv_c + v_c Dp/\gamma}{RT_{ck}} \tag{6}$$

The remaining parameters can be determined using the results of (5) and (6) and the ideal gas equation. The mass of working gas in the heat exchanger spaces is given by

$$m_X = \frac{pV_X}{RT_X} \tag{7}$$

with the appropriate value of k, r, or h, representing the cooler, regenerator, and heater, respectively, substituted in for X. The mass in the expansion space follows as

$$m_e = M - (m_c + m_k + m_r + m_h) \tag{8}$$

where M is the total mass of the working gas inside the Stirling engine. The mass flow between the sections of the engine are given by

$$\begin{aligned} gA_{ck} &= -Dm_c \\ gA_{kr} &= gA_{ck} - \frac{m_k Dp}{p} \\ gA_{rh} &= gA_{kr} - \frac{m_r Dp}{p} \\ gA_{he} &= gA_{rh} - \frac{m_h Dp}{p} \end{aligned} \tag{9}$$

The heat exchanger compartments are assumed to be isothermal. Depending on the accuracy required in the model, the ambient temperature, which affects the cooler temperature, can either be set to a constant value or serve as an input. The heater temperature is supplied from the results of (2), and the regenerator temperature can be found from the heater and cooler temperatures by using the following

$$T_r = \frac{T_h - T_k}{\ln(T_h/T_k)} \tag{10}$$

The temperature of the gas within the working space compartments is found from the ideal gas equation, given by

$$T_{c,h} = \frac{pV_{c,h}}{Rm_{c,h}} \tag{11}$$

The temperature of the gas flowing between the working space volumes and the heat exchangers depends on the direction of mass flow. If the gas is flowing from the compression space to the cooler, gA_{ck} is positive, and thus the interface temperature T_{ck} is equal to the compression space temperature T_c. Otherwise, T_{ck} is equal to the temperature of the cooler T_k. A similar relationship exists for the temperature of the gas flowing between the heater and the expansion space. The gas temperature flowing between the heater and regenerator T_{rh} and the cooler and the regenerator T_{kr} is equal to the corresponding heater or cooler temperature under the assumption of perfect regeneration. The rate of heat transfer in the heat exchanger compartments, given by

$$\begin{aligned} DQ_k &= \frac{V_k Dpc_V}{R} - c_P(T_{ck}gA_{ck} - T_{kr}gA_{kr}) \\ DQ_r &= \frac{V_r Dpc_V}{R} - c_P(T_{kr}gA_{kr} - T_{rh}gA_{rh}) \\ DQ_h &= \frac{V_h Dpc_V}{R} - c_P(T_{rh}gA_{rh} - T_{he}gA_{he}) \end{aligned} \tag{12}$$

significantly affects the energy balance between the absorber and the Stirling engine. As DQ_h increases, more heat is used in powering the Stirling engine, and the temperature starts to decrease on the absorber. Similarly, if too little heat is being absorbed by the Stirling engine, the temperature on the absorber will increase. DQ_h can be controlled by varying the

Stirling engine pressure, where an increase in pressure increases the mass flow through the absorber, thus increasing the heat exchange rate. Conversely, the heat exchange rate decreases for a decrease in pressure.

The power developed by the Stirling engine is directly proportional to the pressure inside the engine. The mechanical power output is given by

$$Power = p(DV_c + DV_e) \tag{13}$$

Similarly, the torque developed is

$$\tau = p\left(\frac{dV_c}{d\phi} + \frac{dV_e}{d\phi}\right) \tag{14}$$

The rotational equation of motion of the Stirling engine shaft is given by

$$\tau = JD\omega + F\omega + \tau_{elec} \tag{15}$$

D. Generator

The generator most commonly used in dish-Stirling systems is the squirrel-cage induction machine, although use of synchronous machines has been reported for remote applications [3]. Squirrel cage machines have the advantages of simple, low-cost, and rugged designs. Typical machine specifications are 480 V, 3 phase, 60 Hz, and 4 poles, with power ratings as discussed above. The induction machine acts as a motor when the shaft speed is below that of the utility supply frequency, and as a generator when the speed is above grid frequency. Only during certain circumstances does the induction machine operate at speeds below synchronous speed, such as during startup of the system when the generator can be used as a starter motor. However, in some cases a separate, smaller starter motor is used to bring the Stirling engine up to operating speed [9]. Nonetheless, during normal operating conditions the speed is maintained above synchronous speed. In addition, the speed of the induction machine must not become too high to avoid damaging the engine components. Under normal operating conditions, the generator has a relatively narrow speed operating region. Fig. 3 shows a typical torque-speed curve of an induction machine, with the operating region labeled as discussed above.

The engine/generator shaft speed is not directly controlled in dish-Stirling systems. The shaft speed is monitored to ensure it remains within the operating range discussed previously. In the event that the shaft speed drops below synchronous speed, a breaker connecting the generator to the utility automatically opens, preventing the system from drawing power. In addition, if a grid fault occurs, resulting in an over-speed condition, a bypass valve is installed as protection to short-circuit the working space volumes, quickly bringing the Stirling engine speed to zero [9]. Models of induction machines are readily available in various power system simulation packages, such as Simulink and PSCAD, and are therefore not discussed here.

V. System Controls

The objective of the temperature control system (TCS) is to maintain the temperature of the absorber at its maximum possible temperature while staying within the thermal limits of the absorber and receiver materials. The temperature is controlled by varying the pressure of the working gas inside the engine. An external high pressure storage tank can supply additional gas to the engine, and thus increase the pressure. During times of high irradiance, the temperature will increase

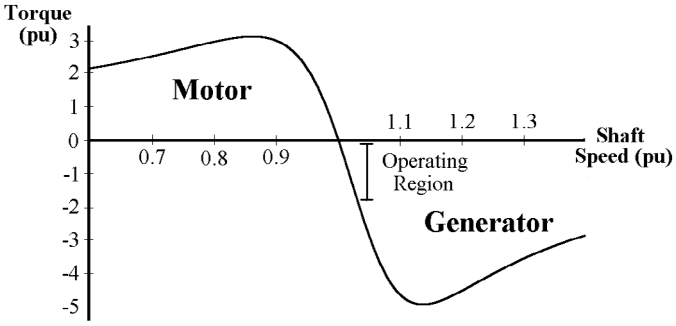

Figure 3. Torque-speed curve of induction machine, with typical operating region when implemented in a dish-Stirling system.

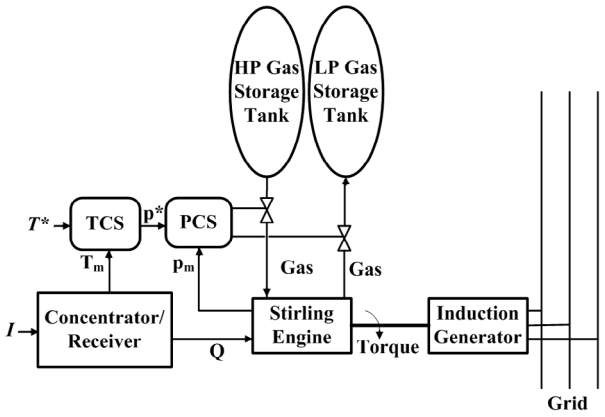

Figure 4. Dish-Stirling control system diagram.

on the absorber surface, so working gas is added from the high pressure storage tank to the engine to regulate the absorber temperature, which also has the effect of increasing the power output of the dish-Stirling system. During times of low irradiance, gas can be removed from the engine by means of a compressor pumping gas back into the high pressure storage tank [10] or by having a separate low pressure tank [11], where a control valve can be opened to allow gas to flow naturally out of the engine. The operation of the control system is illustrated by the block diagram in Fig 4. The TCS measures the absorber temperature and compares it to a reference temperature, and outputs a command pressure to the pressure control system (PCS). Similarly, the PCS measures the pressure inside the engine, and adjusts the valve positions to match the command pressure with the measured pressure. The pressure commanded by the TCS follows a pattern illustrated in Fig. 5. When the measured temperature on the absorber is below the temperature set point T_{SET}, the command pressure remains at its idle point. As the temperature increases above T_{SET}, the command pressure from the TCS increases to regulate the increasing temperature on the absorber. The temperature ΔT_{MAX} defines how much the

absorber temperature can increase above the predefined temperature set point and still be regulated by the PCS. Once the absorber temperature exceeds $T_{SET} + \Delta T_{MAX}$, the pressure inside the Stirling engine is at its maximum, and cannot be increased further to regulate the absorber temperature. Under normal operating conditions, the temperature on the absorber varies from T_{SET} to ΔT_{MAX}, independent of irradiance level. Note that in Fig. 5, the working gas is helium and maximum pressure is 15 MPa, but these parameters may vary among different Stirling engine designs, and simply represent the particular Stirling engine parameters studied in [10].

VI. Simulation Strategy

Referring to Fig. 4, simulation of the dish-Stirling system requires two external inputs: the absorber temperature set point T^* and the instantaneous irradiance I. Initial conditions are required for the crank angle, pressure, compression space

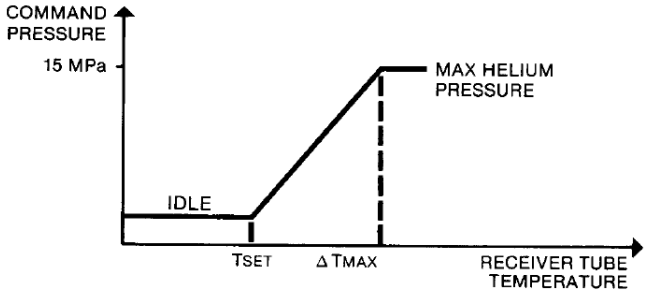

Figure 5. Relationship between absorber temperature and command pressure [10].

mass, the total engine mass, and interface temperatures T_{ck} and T_{he}. The absorber temperature calculated from (2) is used as the heater temperature input to the Stirling engine equations. The working gas quantities are calculated using the Ideal Adiabatic Model equations described above, and the resulting torque developed by the Stirling engine serves as the input to the induction machine model. The induction machine model calculates the shaft speed, from which the crank angle can be determined using the relation

$$\omega = D\phi \tag{16}$$

The flow diagram for the simulations is shown in Fig. 6.

VII. Model Description and Results

A four cylinder Stirling engine is simulated, with the cylinder configuration and drive mechanism shown in Fig. 7. The engine is divided into four quadrants, each quadrant having its own set of heat exchangers. Assuming no leakage past the pistons, the working gas in each quadrant is isolated from the neighboring quadrant. Therefore, each piston is connected to the expansion space of one quadrant and the compression space of the neighboring quadrant. Each quadrant is modeled by the Ideal Adiabatic Analysis described above. The output torque is thus a result of the four quadrant pressures acting on the pistons.

Results of the pressure, temperature, and torque for several revolutions of the crankshaft are shown in Fig. 8. The temperature and pressure of Figs. 8(a) and 8(b) are for one quadrant only, while the torque waveform of Fig. 8(c) is a result of the pressure from all four quadrants acting on the pistons. Set points for the simulation are an irradiance of 1000 W/m^2 and an absorber temperature of 993 degrees Kelvin. The sinusoidal volume variations in the compression and expansion spaces cause periodic oscillations in the engine parameters.

Shown in Fig. 9 are the heater temperature, pressure, and Stirling engine torque as a function of irradiance. The output torque increases, as expected, for increasing irradiance. Two operating regions can be identified by observing the pressure and temperature plots; for irradiance above approximately 250 W/m^2, the heater temperature stays relatively constant and the output torque is proportional to the pressure. For irradiance below 250 W/m^2, the pressure is at its minimum value, and

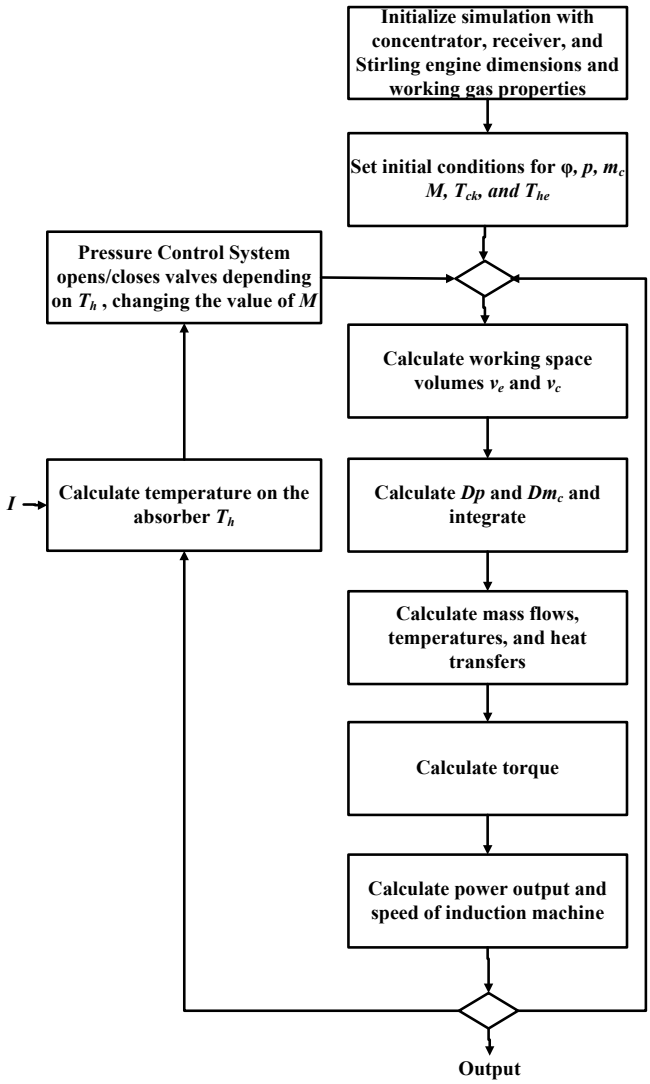

Figure 6. Flow diagram for simulation of a dish-Stirling system.

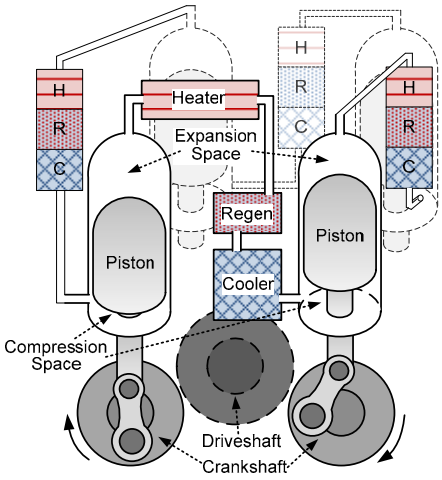

Figure 7. Modeled 4-cylinder engine.

thus the torque produced by the Stirling engine is primarily a function of the heater temperature. The results shown in Fig. 9 verify the operation of the TCS and the PCS, given that after the heater temperature surpasses 993 K, the pressure adjusts to control the heater temperature. However, below the temperature set point of 993 K, the pressure is constant, and thus the heater temperature is a dependent upon the incident solar irradiance.

VIII. Conclusion

The development of the dish-Stirling model in this paper provides a basis for complete dish-Stirling model simulations. Depending on the application, the model may require extension to include more non-ideal characteristics of the dish-Stirling system, including imperfect sun tracking, detailed optical and thermal losses of the receiver, Stirling engine friction losses, pressure drops across Stirling engine compartments, and imperfect regeneration. More detailed models require additional information on dimensions and material characteristics of dish-Stirling components, which are not readily available in current literature.

IX. References

[1] "Tessera Solar and Stirling Energy Systems Unveil World's First Commercial Scale SuncatcherTM Plant, Maricopa Solar, with Utility Partner Salt River Project," Press Release, Tessera Solar. January 22, 2010. URL- http://tesserasolar.com/north-america/pdf/2010_01_22.pdf

[2] Image source: http://en.wikipedia.org/wiki/File:EuroDishSBP_front.jpg

[3] Thomas Mancini, Peter Heller, Barry Butler, et. al, "Dish-Stirling Systems: An Overview of Development and Status," ASME, *Journal of Solar Energy Engineering*, vol. 125, pp. 135-151, May 2003.

[4] William B. Stine and Richard B. Diver, "A Compendium of Solar Dish/Stirling Technology." Sandia National Laboratories, Report SAND93-7026 UC-236, January 1994.

[5] Francois Nepveu, Alain Ferriere, and Francoise Bataille, "Thermal Model of a Dish/Stirling Systems" Elsevier, *Solar Energy*, vol. 83, pp. 81-89, Jan. 2009.

[6] K.O. Lund, "A Direct-Heating Energy-Storage Receiver for Dish-Stirling Solar Energy Systems," ASME, *Journal of Solar Energy Engineering*, vol. 118, pp. 15-19, February 1996.

[7] I. Urieli, "The Ideal Adiabatic Cycle-A Rational Basis for Stirling Engine Analysis," IEEE, *Proceedings of the 17th Intersociety Energy Conversion Engineering Conference*, vol. 4, pp. 1662-1668, 1982. D.G.

[8] Thombare and S.K. Verma, "Technological Development in the Stirling Cycle Engines," Elsevier, *Renewable and Sustainable Energy Reviews*, vol. 12, issue 8, pp. 1-38, Jan. 2008.

[9] J.J. Droher and S.E. Squier, "Performance of the Vanguard Solar Dish-Stirling Engine Module." Electric Power Research Institute, Report EPRI AP-4608, July 1986.

[10] Sten-Hakan Almstrom, Christer Bratt, and Hans-Goran Nelving, "Control Systems for United Stirling 4-95 Engine In Solar Application," United Stirling, *Proceedings of the 16th Intersociety Energy Conversion Engineering Conference*, Aug. 9-14, 1981, Atlanta, GA.

[11] Byron J. Washom, "Vanguard 1 Solar Parabolic Dish-Stirling Engine Module," Advanco Corporation, DOE Contract DE-FC04-82AL16333, Sep.1984.

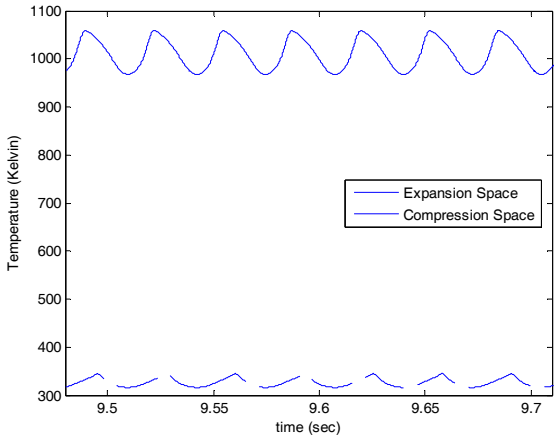

(a)

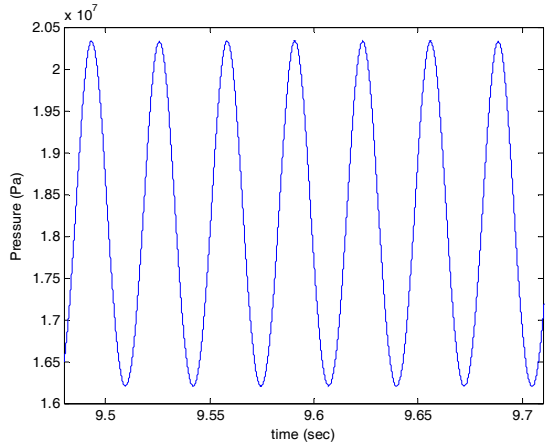

(b)

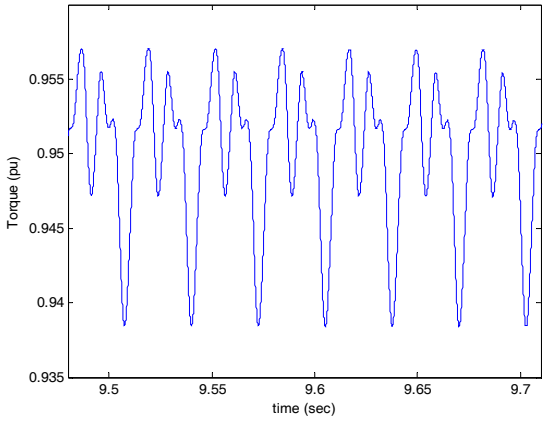

(c)

Figure 8. Plots of (a) expansion and compression space temperature, (b) pressure, and (c) engine torque for several revolutions of the crankshaft.

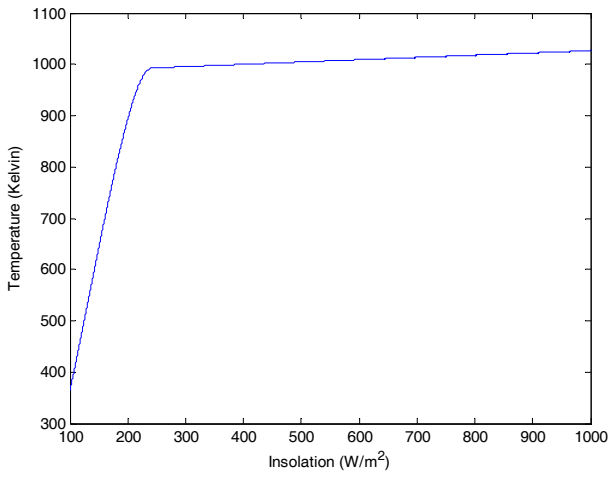

(a)

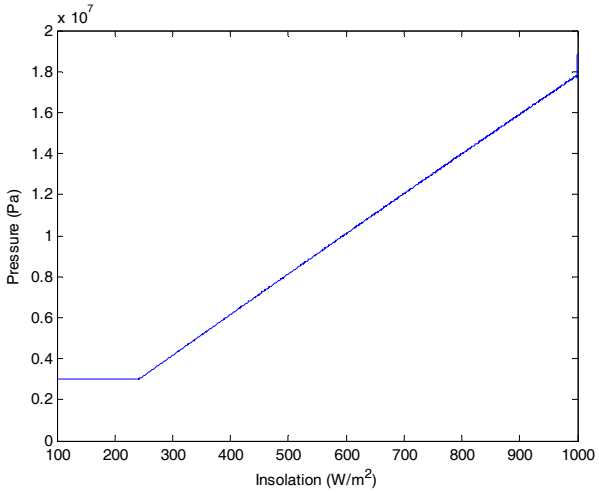

(b)

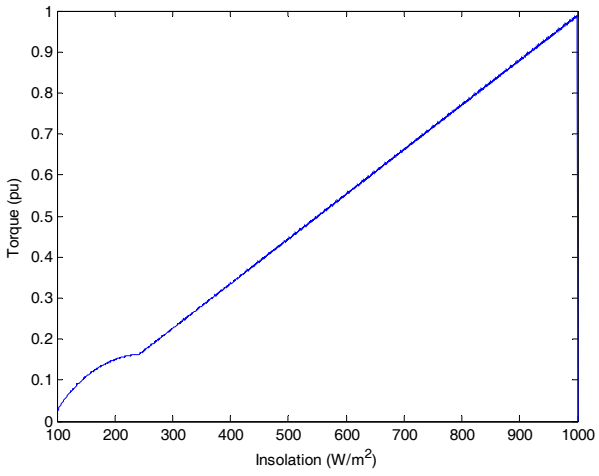

(c)

Figure 9. Variation of (a) heater temperature, (b) average engine pressure, and (c) engine torque versus solar irradiance.

X. Biographies

Dustin Howard (M'09) is from Douglas, GA, U.S. and is currently a graduate student at the Georgia Institute of Technology. He received his Bachelors Degree in Electrical Engineering in 2008, where his primary focus was in electric power and control systems. He is currently pursuing a Masters Degree in the same disciplines.

Ronald G. Harley (M'77–SM'86–F'92) received the M.Sc.Eng. degree in electrical engineering from the University of Pretoria, Pretoria, South Africa, in 1965, and the Ph.D. degree from London University, London, U.K., in 1969.

He is currently the Duke Power Company Distinguished Professor with the School of ECE, Georgia Tech, Atlanta. He has coauthored around 400 papers in refereed journals and conference proceedings and holds three patents.

Dr. Harley was one of the IEEE Industry Applications Society's six Distinguished Lecturers during 2000–2001. He was the recipient of the Cyril Veinott Electromechanical Energy Conversion Award in 2005 from the IEEE Power Engineering Society and the Richard Harold Kaufmann Technical Field Award in 2009 from the IEEE Industry Applications Society.